DALTON
FULL PAPER

Solid state coordination chemistry: ligand influences on the structures of one-dimensional copper(I) cyanide–organodiimine solids

Douglas J. Chesnut, Anakarin Kusnetzow, Robert Birge and Jon Zubieta *

Department of Chemistry, Syracuse University, Syracuse, NY 13244, USA

Received 4th January 2001, Accepted 20th June 2001
First published as an Advance Article on the web 21st August 2001

The structural consequences of introducing sterically demanding substituents have been investigated for composite organic–inorganic materials of the copper cyanide–organodiimine system. The hydrothermal reactions of copper(I) cyanide and KCN, with the appropriate chelating organodiimine ligands yield a series of one-dimensional copper cyanide chains decorated either with linear {(LL)Cu(CN)} (LL = organodiimine) side chains or with diimine ligands bound directly to the copper sites of the parent chain. The structures of $[Cu_3(CN)_3(2,2'\text{-bpy})]$ (**1**) (2,2′-bpy = 2,2′-bipyridine) and $[Cu_3(CN)_3(phen)]$ (**2**) (phen = 1,10-phenanthroline) are similar to that of the previously reported $[Cu_4(CN)_4(biquin)]$ (biquin = 2,2′-biquinoline), exhibiting the characteristic one-dimensional {Cu(CN)} chain with diimine–copper cyanide side arms. In contrast, the structures of $[Cu_3(CN)_3(biquin)_2]$ (**3**), $[Cu_2(CN)_2(dpbp)]$, (**4**) (dpbp = 4,4′-diphenyl-2,2′-bipyridine), and [Cu(CN)(dpphen)] (**5**) (dpphen = 4,7-diphenyl-1,10-phenanthroline) are characterized by direct attachment of the organodiimine ligand to the copper cyanide chain.

Introduction

Transition metal cyanides[1] are a versatile family of inorganic materials with varied physical properties, giving rise to applications as inclusion compounds,[2,3] catalysts,[4] zeolitic materials,[5] and molecular-based magnets.[6] Copper(I) cyanide is of fundamental and practical interest in cyano-Gilman chemistry,[7] as a precursor for open-framework materials,[8–12] and in the synthesis of superconducting materials.[13]

One approach to the design of new materials or for the manipulation of the microstructures of inorganic phases exploits the incorporation of organic components.[14] The resultant organic–inorganic hybrid material combines the unique features of both constituents in fashioning the architecture of a material with composite or even novel physical properties.[15] Copper(I) cyanide is an attractive material from this viewpoint of "crystal engineering"[16,17] since the $\{Cu(CN)\}_n$ chain substructure appears to be particularly versatile in accommodating a wide range of ligands and geometric constraints.

In the course of our investigations of one- and two-dimensional organic–inorganic hybrid structures derived from $\{Cu(CN)\}_n$ chains,[9–12] the prototypical one-dimensional material $[Cu_4(CN)_4(biquin)]$ (biquin = biquinoline) was characterized. As an extension of this work, the structural consequences of introducing chelating organodiimine ligands with varying degrees of steric bulk into the Cu(CN) structure was investigated using the ligand set of Scheme 1. The hydrothermal reactions of Cu(CN) with these ligands yielded two subsets of materials: (i) one-dimensional {Cu(CN)} chains decorated with organodiimine–copper cyanide side arms $[Cu_3(CN)_3(2,2'\text{-bpy})]\cdot 0.1H_2O$ ($\mathbf{1}\cdot 0.1H_2O$) and $[Cu_3(CN)_3(phen)]$ (**2**) and (ii) {Cu(CN)} chains with the organodiimine coordinated directly to Cu(I) sites of the parent chain, $[Cu_3(CN)_3(biquin)_2]$ (**3**), $[Cu_2(CN)_2(dpbp)]$ (**4**), and [Cu(CN)(dpphen)] (**5**).

Experimental

Reagents were purchased from Aldrich Chemical Co. and used without further purification. All syntheses were carried out in 23 mL polytetrafluoroethylene-lined Parr stainless steel containers or borosilicate tubes under autogenous pressure. The reactants were stirred briefly before heating. Water was distilled above 3.0 Ω in-house using a Barnstead Model 525 Biopure Distilled Water Center.

Syntheses

$[Cu_3(CN)_3(2,2'\text{-bpy})]\cdot 0.1H_2O$ ($\mathbf{1}\cdot 0.1H_2O$). A mixture of CuCN (0.372 g, 4.15 mmol), KCN (0.275 g, 4.22 mmol), 1,2,4-triazole (0.068 g, 0.98 mmol), 2,2′-bipyridine (0.147 g, 0.94 mmol) and H_2O (11.26 g, 626 mmol) in a heavy-walled borosilicate tube 14 in long and 0.5 in inner diameter was heated at 165 ± 5 °C for 190 h. The tube was then cooled to room temperature over a 4 h period. The resultant mixture of black powder and small pale red crystals was separated mechanically. The yield of red crystals was 25% based on copper. The presence of water of crystallization was confirmed by FTIR-microscopy.

$[Cu_3(CN)_3(phen)]$ (2). A mixture of CuCN (0.361 g, 2.03 mmol), KCN (0.064 g, 1.0 mmol), 1,10-phenanthroline (0.179 g, 0.99 mmol) and H_2O (5.00 mL, 278 mmol) was heated at 170 ± 5 °C for 96 h in a 23 mL Parr acid digestion bomb. After cooling, yellow crystals of **2** were recovered by filtration (Yield: 45%).

$[Cu_3(CN)_3(biquin)_2]$ (3). A mixture of CuCN (0.534 g, 5.99 mmol), $Cu(NO_3)_2\cdot 2.5H_2O$ (0.232 g, 1.0 mmol), 2,2′-biquinoline (biquin: 0.157 g, 1.01 mmol) and H_2O (5.20 mL, 289 mmol) was heated for 86.5 h at 170 ± 5 °C. A mixture of red crystals of **3** and yellow crystals of $[Cu_4(CN)_4(biquin)]$ were collected by filtration and separated mechanically (Yield of **3**: 20%).

$[Cu_2(CN)_2(dpbp)]$ (4). A mixture of CuCN (0.363 g, 4.05 mmol), KCN (0.065 g, 1.0 mmol), 4,4′-diphenyl-2,2′-bipyridine (dpbp: 0.307 g, 1.0 mmol) and H_2O (5.00 mL, 278 mmol) was heated at 170 ± 5 °C for 96 h in a 23 mL Parr acid digestion bomb. After cooling, dark red crystals of **4** were recovered in 65% yield.

DOI: 10.1039/b100392p

Table 1 Summary of crystal data for the structural determinations of $[Cu_3(CN)_3(2,2'\text{-bpy})]\cdot0.1H_2O$ (**1**·0.1H$_2$O), $[Cu_3(CN)_3(phen)]$ (**2**), $[Cu_3(CN)_3(biquin)_2]$ (**3**), $[Cu_2(CN)_2(dpbp)]$ (**4**) and $[Cu(CN)(dpphen)]$ (**5**)

	1·0.1H$_2$O	**2**	**3**	**4**	**5**
Formula	$C_{13}H_8Cu_3N_5\cdot0.1H_2O$	$C_{15}H_8Cu_3N_5$	$C_{39}H_{24}Cu_3N_7$	$C_{24}H_{16}Cu_2N_4$	$C_{25}H_{16}CuN_3$
FW	426.46	448.88	781.27	487.49	421.95
Space group	$P2_1/n$	$P2_1/c$	$C2/m$	$P2_1/c$	$Cmc2_1$
T/K	293(2)	293(2)	293(2)	293(2)	293(2)
a/Å	10.128(2)	9.6979(2)	13.667(2)	12.112(2)	25.534(1)
b/Å	13.659(3)	23.5984(4)	15.330(2)	9.941(1)	9.710(1)
c/Å	11.012(2)	6.8989(1)	7.848(2)	16.308(3)	7.638(1)
β/°	109.663(5)	99.26(1)	96.751(2)	93.743(5)	90.00
V/Å^3	1434.6(5)	1558.26(5)	1632.80(5)	1959.5(7)	1893.7(1)
Z	4	4	2	4	4
D_c/g cm^{-3}	1.975	1.913	1.589	1.652	1.480
μ/cm^{-1}	44.04	40.60	19.77	21.89	11.69
$R1$	0.0271	0.0507	0.0343	0.0560	0.0781
$wR2$	0.0694	0.1089	0.0734	0.0916	0.1343

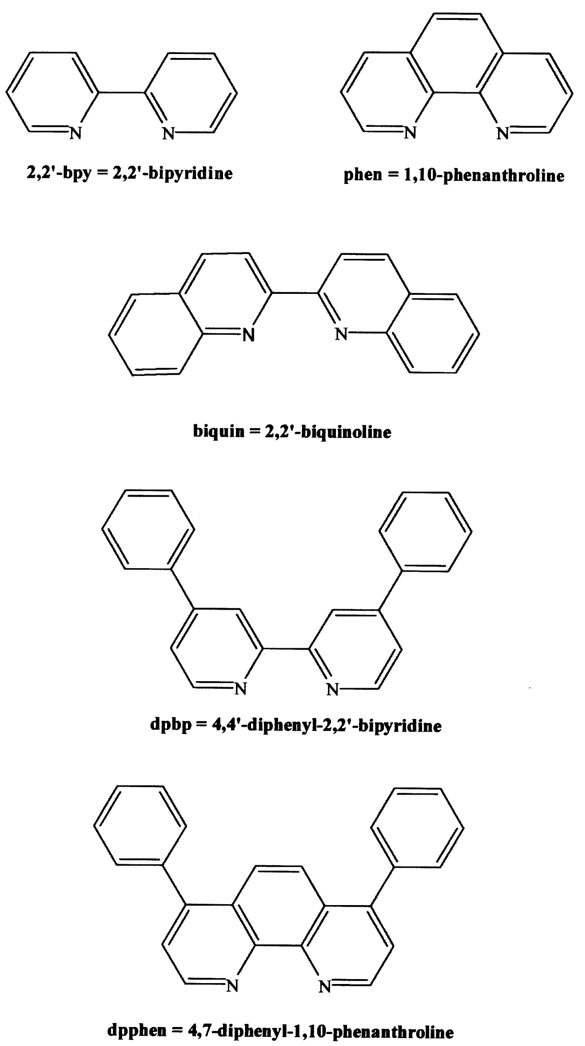
2,2'-bpy = 2,2'-bipyridine

phen = 1,10-phenanthroline

biquin = 2,2'-biquinoline

dpbp = 4,4'-diphenyl-2,2'-bipyridine

dpphen = 4,7-diphenyl-1,10-phenanthroline

Scheme 1

Table 2 Selected bond lengths (Å) and angles (°) for $[Cu_3(CN)_3(2,2'\text{-bpy})]\cdot0.1H_2O$ (**1**·0.1H$_2$O)

Cu1–X3	1.848(2)	Cu3–X6	1.855(2)
Cu1–X2	1.848(2)	Cu3–N8	2.007(2)
Cu1–Cu3A	2.876(1)	Cu3–N7	2.060(2)
Cu2–X1A	1.907(2)	X1–X2	1.152(3)
Cu2–X4	1.928(2)	X3–X4	1.159(3)
Cu2–X5	1.946(2)	X5–X6	1.154(3)
X3–Cu1–X2	176.30(9)	X1A–Cu2–X4	123.60(8)
X1A–Cu2–X5	123.42(8)	X4–Cu2–X5	112.93(8)
N6–Cu3–N8	151.02(9)	X6–Cu3–N7	127.98(8)
N8–Cu3–N7	80.95(7)	X1–X2–Cu1	177.4(2)
X4–X3–Cu1	176.3(2)	X3–X4–Cu2	179.7(2)
X6–X5–Cu2	169.8(2)	X5–X6–Cu3	173.8(2)
X2–X1–Cu2A	176.6(2)		

[Cu(CN)(dpphen)] (5). A mixture of CuCN (0.360 g, 4.02 mmol), $Cu(NO_3)_2\cdot2.5H_2O$ (0.326 g, 1.40 mmol), 4,7-diphenyl-1,10-phenanthroline (dpphen: 0.328 g, 1.06 mmol) and H_2O (5.00 mL, 278 mmol) was heated at 170 ± 5 °C for 96 h. After cooling, dark red crystals of **5** were collected in 10% yield.

Crystal structure determinations

Single crystal diffraction data for **1**–**5** were measured using a Bruker P4 diffractometer equipped with the SMART system[18] and using Mo-Kα radiation ($\lambda = 0.71073$ Å). All data sets were corrected for Lorentz and polarization effects, and absorption corrections were made using SADABS.[19] The structure solutions and refinements were carried out using SHELXL96.[20] All structures were solved using direct-methods and all of the non-hydrogen atoms were located from the initial solution or from subsequent electron density difference maps during the initial stages of the refinement. After locating all of the non-hydrogen atoms in each structure the models were refined against F^2, first using isotropic and finally anisotropic thermal displacement parameters, until the final value of σ/Δ_{max} was less than 0.001. The positions of the hydrogen atoms were then calculated and fixed, and a final cycle of refinements was performed until σ/Δ_{max} was again less than 0.001.

The crystal data for **1**–**5** are summarized in Table 1. Selected bond lengths and angles for the structures of **1**–**5** are presented in Tables 2–6.

The cyano groups of compounds **1**–**5** were crystallographically disordered. The positions of the N atoms and the C atoms of the cyano groups were modeled with each position having an occupancy of 50% of each atom type. The temperature factors were then simultaneously refined.

CCDC reference numbers 156995–156999.

See http://www.rsc.org/suppdata/dt/b1/b100392p/ for crystallographic data in CIF or other electronic format.

FTIR spectroscopy

Fourier-transform infrared spectra were obtained using a Nicolet Nic-Plan microscope coupled to a Nicolet Magna IR750. Single crystals of the copper cyanide sample were selected based on thickness and the absence of inclusions or surface debris. The selected crystals were mounted on CaF_2 windows (4000–1100 cm^{-1}), and images were focused using a 32X IR objective lens. Transmission spectra were collected and averaged (5/6 scans) at a resolution of 2 cm^{-1}; the area

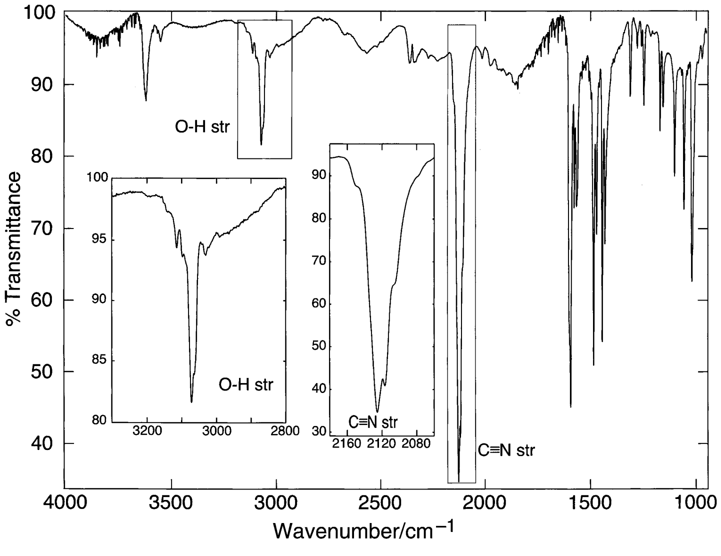

Fig. 1 The infrared spectrum of $[Cu_3(CN)_3(2,2'\text{-bpy})]\cdot 0.1H_2O$ (**1**·$0.1H_2O$).

Table 3 Selected bond lengths (Å) and angles (°) for $[Cu_3(CN)_3(phen)]$ (**2**)

Cu1–X1	1.876(7)	Cu3–X5	1.862(5)
Cu1–N8	2.000(5)	Cu3–X4	1.868(5)
Cu1–N7	2.103(5)	X1–X2	1.150(7)
Cu2–X6	1.905(5)	X5–X5A	1.17(1)
Cu2–X3	1.918(6)	X6–X6A	1.17(1)
Cu2–X2	1.983(5)	Cu2–Cu3	2.852(1)
X1–Cu1–N8	153.3(2)	X1–Cu1–N7	123.0(2)
N8–Cu1–N7	83.0(1)	X6–Cu2–X3	130.2(2)
X6–Cu2–X2	117.5(2)	X3–Cu2–X2	112.2(2)
X5–Cu3–X4	159.5(2)	X2–X1–Cu1	69.8(5)
X1–X2–Cu2	163.4(4)	X4–X3–Cu2	174.3(5)
X3–X4–Cu3	175.8(5)	X5A–X5–Cu3	178.7(7)
X6A–X6–Cu2	177.2(7)		

Table 4 Selected bond lengths (Å) and angles (°) for $[Cu_3(CN)_3(biquin)_2]$ (**3**)

Cu2–X1	1.828(3)	Cu1–N4	2.094(1)
Cu1–X2	1.902(4)	X1–X2	1.157(4)
Cu1–X3	1.950(3)	X3–X3A	1.161(6)
X1A–Cu2–X1	180.00(0)	X2–Cu1–X3	129.3(1)
X2–Cu1–N4	115.87(9)	X3–Cu1–N4	102.76(8)
X2–Cu1–N4A	115.87(9)	X3–Cu1–NA	102.76(8)
X4–Cu1–X4A	77.10(1)	X1–X2–Cu1	178.0(3)
X3A–X3–Cu1	173.4(4)		

Table 5 Selected bond lengths (Å) and angles (°) for $[Cu_2(CN)_2(dpbp)]$ (**4**)

Cu1–X1	1.911(4)	Cu2–X4	1.834(3)
Cu1–X2	1.966(3)	Cu2–X3	1.854(4)
Cu1–N6	2.089(3)	X1–X4A	1.162(5)
Cu1–N5	2.109(3)	X2–X3	1.159(5)
X1–Cu1–X2	120.1(1)	X1–Cu1–N6	127.2(1)
X2–Cu1–N6	100.1(1)	X1–Cu1–N5	108.2(1)
X2–Cu1–N5	116.1(1)	N6–Cu1–N5	78.7(1)
X4–Cu2–X3	175.5(1)	X4A–X1–Cu1	173.7(4)
X3–X2–Cu1	168.3(3)	X2–X3–Cu2	171.9(4)
X1A–X4–Cu2	173.7(3)		

scanned was 10 microns in diameter. The detector used for data collection was a liquid N_2 cooled MCT-A detector. The Omnic 3.1 software was used for data collection and processing. Plots were generated using IGOR Pro 3.02 and Adobe Illustrator® 7.0 software packages.

Table 6 Selected bond lengths (Å) and angles (°) for $[Cu(CN)(dpphen)]$ (**5**)

Cu1–X1	1.905(8)	Cu1–N3	2.075(3)
Cu1–X2	1.918(7)	X1–X2A	1.181(8)
X1–Cu1–X2	105.9(3)	X1–Cu1–N3	116.4(2)
X2–Cu1–N3	118.7(1)	N3–Cu1–N3A	79.8(1)
X2A–X1–Cu1	163.6(6)	X1A–X2–Cu1	173.3(5)

Results and discussion

While inorganic solid state materials have been conventionally prepared by high temperature techniques, the incorporation of organic subunits into the structure of the hybrid material requires lowering the reaction temperature to ensure the structural integrity of the organic molecule. Consequently, the synthesis of such organic–inorganic hybrid materials requires a shift from the thermodynamic to the kinetic regime. A variety of *chimie douce* or soft chemical techniques have been described which allow access to such metastable species.

The hydrothermal method[21] has been used successfully in the organic-directed crystallization of a variety of materials including zeolites, mesoporous materials of the MCM-41 class, transition metal oxides, phosphates, organophosphonates, and cyanides. The syntheses of **1**–**4** exploited hydrothermal conditions to those previously employed by us in the preparation of $[Cu_4(CN)_4(biquin)]$ and other copper(I) cyanide–organoimine materials.[22–24]

Two features of the syntheses are noteworthy: (i) KCN is routinely added to ensure crystal growth; and (ii) regardless of the oxidation state of the copper starting material, the products contain copper exclusively in the +1 oxidation state, which is consistent with the stability of Cu(I) cyanide species with respect to Cu(II) materials at elevated temperatures and pressures.[25] Since the K^+ cation does not appear in the products, the KCN may be acting as a mineralizer or solubilizing agent for the one-dimensional $\{Cu(CN)\}_\infty$ subunits.

In a typical reaction, Cu(CN), KCN, 2,2′-bipyridine and H_2O in the mole ratio 6.0 : 1.0 : 1.0 : 290 were heated at 165 ± 5 °C for 190 h to give red crystals of $[Cu_3(CN)_3(2,2'\text{-bpy})]\cdot 0.1H_2O$ (**1**·$0.1H_2O$) in 25% yield. The infrared spectrum of this material exhibited bands at 2125 and 2110 cm^{-1} attributed to ν(CN) and a feature at 3084 cm^{-1} consistent with the presence of water of crystallization (Fig. 1). Three coordinate copper cyanide structures have also been reported for $KCu(CN)_2$,[26] $K[Cu_2(CN)_3]\cdot H_2O$[27] and $NaCu(CN)_2\cdot 2H_2O$,[28] as well as $(NBu_4)[Cu(CN)Br]$[29] and $[Cu_3(CN)_3(hmta)_2]$ (hmta = hexamethylenetetramine).[30]

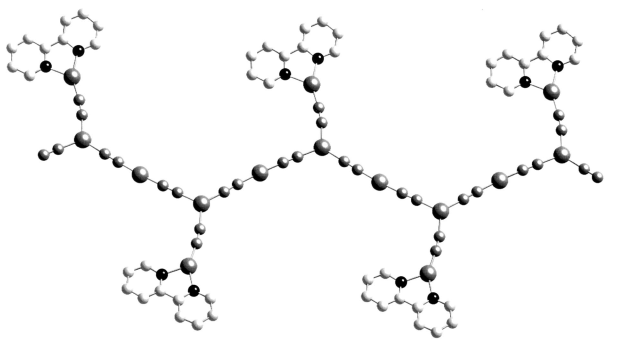

Fig. 2 A view of the one-dimensional structure of $[Cu_3(CN)_3(2,2'\text{-bpy})]\cdot 0.1H_2O$. The water molecules of crystallization have been omitted for clarity.

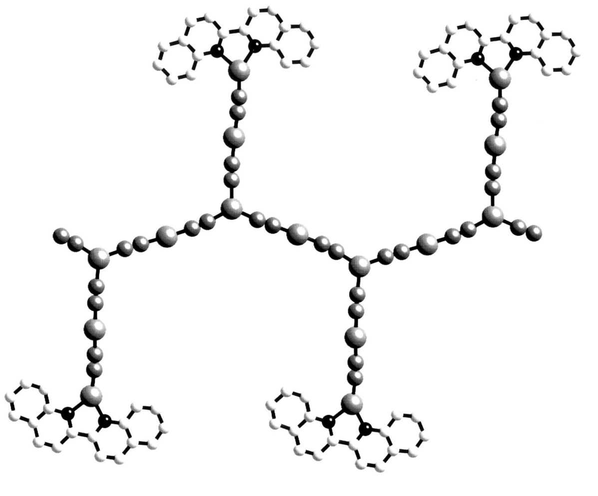

Fig. 3 The one-dimensional structure of $[Cu_4(CN)_4(\text{biquin})]$.

As shown in Fig. 2, the structure of $[Cu_3(CN)_3(2,2'\text{-bpy})]\cdot 0.1H_2O$ ($\mathbf{1}\cdot 0.1H_2O$) exhibits a backbone constructed from a zig-zag {Cu(CN)} chain. Alternate Cu(I) sites in the chain are two coordinate, while the remaining sites exhibit trigonal-planar $\{Cu(CN)_3\}$ geometry, with two cyano groups participating in bridging within the parent chain while the third projects from the chain to link to a {Cu(bpy)} side arm. The structure of **1** is reminiscent of that of the previously reported $[Cu_4(CN)_4(\text{biquin})]$,[9] shown in Fig. 3. However, this latter material exhibits an extended side arm with an additional {Cu(CN)} subunit linking the {(biquin)Cu(CN)} arm to the parent chain.

It is noteworthy that small variations in reaction conditions for the Cu(I)/CN/2,2′-bipyridine system results in profound structural changes. Thus, changes in reaction stoichiometries were shown to yield two-dimensional phases, $[\{Cu_2(2,2'\text{-bpy})_2(CN)\}Cu_5(CN)_6]$ and $[\{Cu_2(2,2'\text{-bpy})_2(CN)\}_2Cu_5(CN)_7]$. Curiously, in these cases, the organodiimine participates in bonding to the $\{Cu_2(2,2'\text{-bpy})_2(CN)\}^+$ molecular cation exclusively. Consequently, the two-dimensional substructures are constructed from fused $\{Cu(CN)\}_n$ rings and contain no directly bound bipyridine.

The structure of $[Cu_3(CN)_3(\text{phen})]$ (**2**) is similar to that of **1**, as shown in Fig. 4. The most significant structural contrast between **1** and **2** is the angle at the two-coordinate Cu(I) sites, which is 176.30(9)° in **1** but deviates significantly from linearity in **2** [159.5(2)°]. While the bipyridyl rings and the {Cu(CN)} chains of **1** produce a planar assembly, the chain folding in **2** results in the disposition shown in Fig. 4.

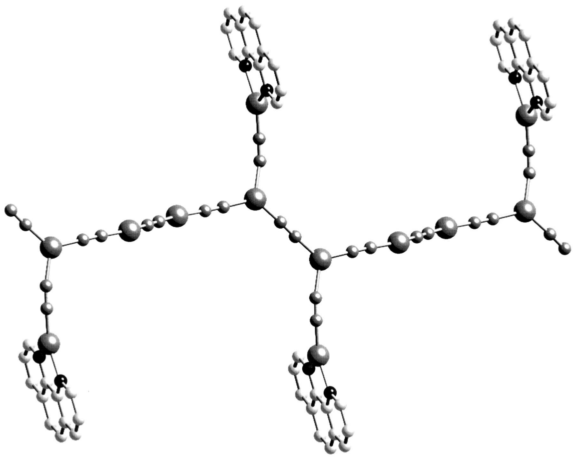

Fig. 4 A view of the structure of $[Cu_3(CN)_3(\text{phen})]$ (**2**).

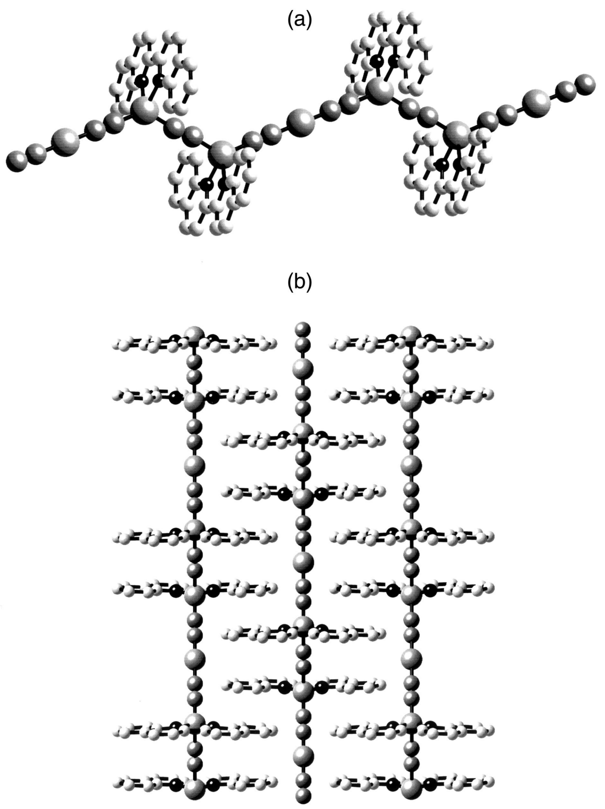

Fig. 5 (a) The chain structure of $[Cu_3(CN)_3(\text{biquin})_2]$ (**3**). (b) A view of the structure of **3** normal to the crystallographic *ab*-plane.

In contrast to the structures of **1**, **2** and $[Cu_4(CN)_4(\text{biquin})]$, the one-dimensional structure of $[Cu_3(CN)_3(\text{biquin})_2]$ (**3**), shown in Fig. 5, does not exhibit side arms, but rather has the organodiimine ligand directly bound to the parent chain. Consequently, one copper site exhibits linear coordination, while the second exhibits highly distorted tetrahedral geometry through coordination to two cyano groups and the nitrogen donors of the biquinoline ligand. A curious feature of the structure is the propagation pattern of two- and four-coordinate sites along the chain. In structures **1**, **2** and $[Cu_4(CN)_4(\text{biquin})]$, the two-coordinate (A) and three-coordinate (B) copper sites repeat in an alternating A–B–A–B pattern. In contrast, in **3**, the two-coordinate (A) and four-coordinate (C) copper sites exhibit an A–C–C–A–C–C pattern. One consequence of this repeat pattern is to force the biquinoline rings on adjacent copper sites into a parallel orientation to relieve steric interactions. As a result, the ligand rings are nearly normal to the direction of propagation of the zig-zag {Cu(CN)} chains. As shown in Fig. 5(b), rings on adjacent chains interdigitate to give a pattern of inorganic chains and organic regions between chains.

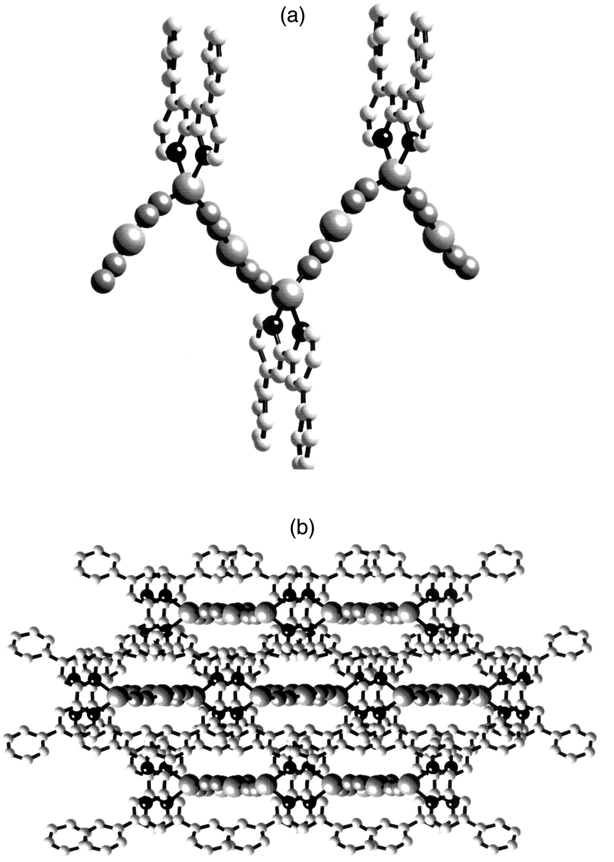

Fig. 6 (a) A view of a single chain of [$Cu_2(CN)_2$(dpbp)] (**4**). (b) A view of the structure of **4** normal to the crystallographic *ab*-plane.

The one-dimensional structure of [$Cu_2(CN)_2$(dpbp)] (**4**), shown in Fig. 6, also exhibits the ligand bound directly to a copper site of the parent chain. However, in this case, the A–C–A–C pattern of alternating two-coordinate (A) and four-coordinate (C) copper sites is observed, in contrast to the A–C–C–A–C–C pattern of **3**. Once again, the rings on adjacent chains interdigitate, resulting in a stacking pattern which generates channels occupied by the {Cu(CN)} chains, shown in Fig. 6(b).

The structure of [Cu(CN)(dpphen)] (**5**), shown in Fig. 7, consists of a one-dimensional {Cu(CN)} chain with a dpphen ligand coordinated to every copper site. Thus, the coordination in this case is exclusively distorted tetrahedral. The (cyanide X)–Cu–(cyanide X) valence angle is only 105.9(3)°, giving rise to a severely puckered chain.

The ligands on adjacent chains interdigitate, as shown in Fig. 7(b), to produce layers of chains when viewed normal to the crystallographic *ab*-plane. The phenyl substituents are rotated by 44° relative to the 1,10-phenanthroline ring, and consequently rings from adjacent "layers" cannot stack or interdigitate. This results in the structural profile of Fig. 7(c) with "layers" separated by phenyl residues projecting into the interlamellar space.

The prevalence of {Cu(CN)} chain motifs in the Cu(I) cyanide chemistry is not unexpected, as spectroscopic evidence is consistent with a one-dimensional structure for [Cu(CN)] itself.[31] The structural systematics of this work support this model.

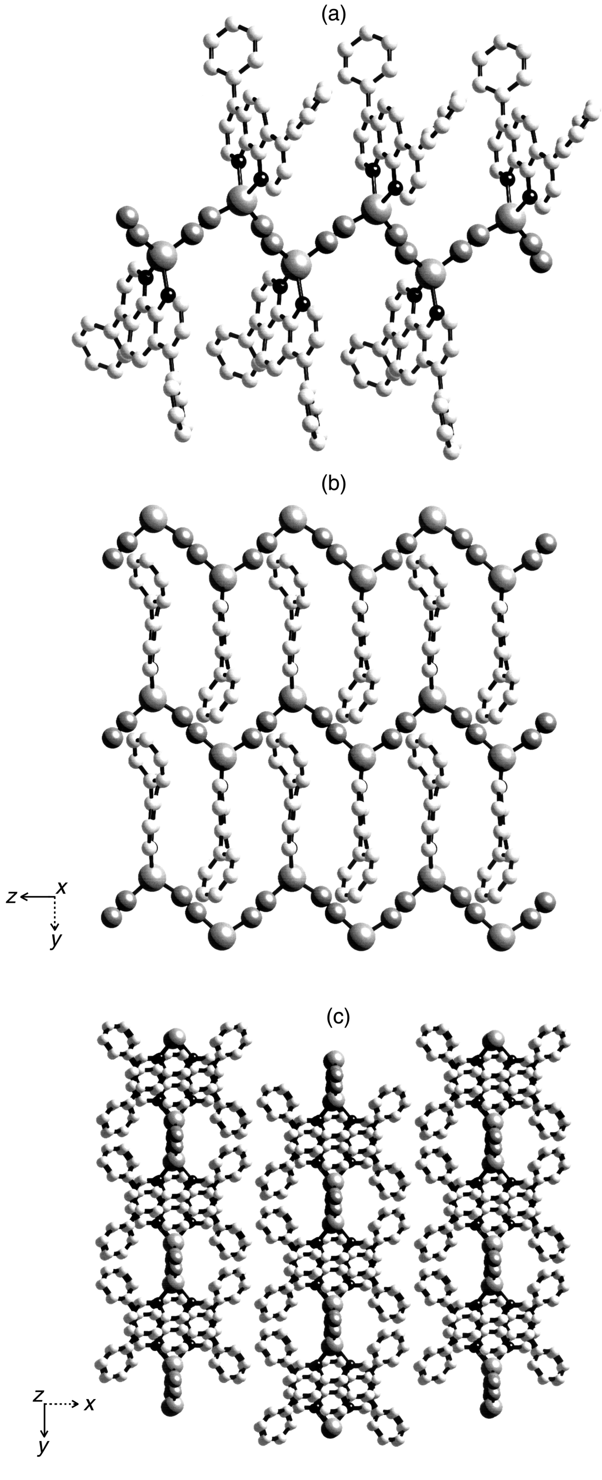

Fig. 7 (a) A view of the chain structure of [Cu(CN)(dpphen)] (**5**). (b) A view of the structure of **5** normal to the crystallographic *bc*-plane. (c) A view of the structure of **5** normal to the *ab*-plane.

Conclusions

Hydrothermal synthesis has been exploited to prepare a series of five one-dimensional phases of the Cu(I)/CN/organodiimine family. In terms of gross geometry two structural subtypes are evident: (i) $\{Cu(CN)\}_n$ chains decorated with {(LL)Cu(CN)} (LL = organodiimine) side arms for [$Cu_3(CN)_3$(2,2′-bpy)] (**1**) and [$Cu_3(CN)_3$(phen)] (**2**); and (ii) {Cu(CN)} chains with the organodiimine ligand coordinated to Cu sites of the parent chain in [$Cu_3(CN)_3(biquin)_2$] (**3**), [$Cu_2(CN)_2$(dpbp)] (**4**) and [Cu(CN)(dpphen)] (**5**). It is noteworthy that structures analogous to those of **3**–**5** which incorporate 2,2′-bipyridine and 1,10-phenanthroline have been proposed,[32] and that the crystal structure of [Cu(CN)(phen)] has been reported.[33] A curious feature of this latter subset of materials (**3**–**5**) is the variation in Cu : CN : LL ratios of 3 : 3 : 2, 2 : 2 : 1, 1 : 1 : 1 for **3**, **4** and **5**, respectively, a characteristic reflected in their structural

Table 7 A comparison of structural motifs for the one-dimensional copper(I) cyanide structures of this study

	X–Cu–X valence angle/°				
	A Site	B Site	C Site	Repeat motifs	Side arm
$[Cu_3(CN)_3(2,2'\text{-bpy})]$ (**1**)	176.30(9)	123.60(8)	—	A–B–A–B	(bpy)Cu(CN)
$[Cu_3(CN)_3(phen)]$ (**2**)	159.5(2)	130.1(2)	—	A–B–A–B	(phen)Cu(CN)
$[Cu_4(CN)_4(biquin)]$	176.0(1)	128.2(1)	—	A–B–A–B	$(biquin)Cu_2(CN)_2$
$[Cu_3(CN)_3(biquin)_2]$ (**3**)	180.0	—	129.3(7)	A–C–C–A–C–C	None
$[Cu_2(CN)_2(dpbp)]$ (**4**)	175.5(1)	—	120.1(1)	A–C–A–C	None
[Cu(CN)(dpphen)] (**5**)	—	—	105.9(3)	C–C–C	None

motifs, as noted in Table 7. Thus, compound **3** exhibits an A–C–C–A–C–C chain repeat, compound **4** an A–C–A–C repeat, and compound **5** simply C–C–C. While the crystal packing in **3**–**5** reflects steric influences of the ligand substituents, it is not at all clear that a given ligand must limit the structural chemistry to the phase observed in this study. For example, there would appear to be no fundamental constraint to the isolation in the Cu/CN/biquinoline family of materials of stoichiometries $[Cu_2(CN)_2(biquin)]$ and [Cu(CN)(biquin)] which are related structurally to **4** and **5**. The existence of both $[Cu_4(CN)_4(biquin)]$ and $[Cu_3(CN)_3(biquin)_2]$ would suggest that other phases may be accessed under the appropriate hydrothermal conditions. Similarly, the Cu/CN/bpy and Cu/CN/phen families should find expansion to one-dimensional materials of the type $[Cu_x(CN)_x(LL)_y]$ where x and y are not limited to 3 and 1, respectively. However, the hydrothermal parameter space is vast, and it may prove challenging to locate the sets of conditions which favor such metastable species.

Despite such reservations, organic components may be introduced into the synthesis of solid state inorganic materials to provide a powerful method for structural manipulations and modification. While predictability of structure remains an elusive goal in such organic–inorganic composite materials, this observation reflects the compositional and structural versatility of inorganic materials. Consequently, the exploration of the structure-determining role of organic subunits in solid inorganic materials remains a challenging field requiring considerable development of structure–property relationships exploiting an essentially empirical approach.

Acknowledgements

This work was supported by a grant from the National Science Foundation (CHE 9987471), NIH (GM-34548), and the W. M. Keck Foundation.

References

1 T. Iwamoto, in *Comprehensive Supramolecular Chemistry*, ed. D. D. MacNcol, F. Toda and R. Bishop, Pergamon Press, Oxford, 1996, vol. 6, ch. 19, p. 643.

2 K. R. Dunbar and R. A. Heintz, *Prog. Inorg. Chem.*, 1997, **45**, 283.

3 T. Iwamoto, *J. Inclusion Phenom.*, 1996, **4**, 61.

4 W. P. Fehlhammer and M. Fritz, *Chem. Rev.*, 1993, **93**, 1243.

5 C. Janiak, *Angew. Chem., Int. Ed. Engl.*, 1997, **36**, 1431 and references therein.

6 S.-W. Zhang, D.-G. Fu, W.-Y Sun, Z. Hu, K.-B. Yu and W.-X Tang, *Inorg. Chem.*, 2000, **39**, 1142 and references therein.

7 B. H. Lipshutz, J. A. Sclafani and T. Takanami, *J. Am. Chem. Soc.*, 1998, **120**, 4021.

8 L. C. Brousseau, D. Williams, J. Kouvetakis and M. O'Keefe, *J. Am. Chem. Soc.*, 1997, **119**, 6292.

9 D. J. Chesnut and J. Zubieta, *Chem. Commun.*, 1998, 1707.

10 D. J. Chesnut, A. Kusnetzow and J. Zubieta, *J. Chem. Soc., Dalton Trans.*, 1998, 4081.

11 D. J. Chesnut, A. Kusnetzow, R. R. Birge and J. Zubieta, *Inorg. Chem.*, 1999, **38**, 2663.

12 D. J. Chesnut, A. Kusnetzow, R. Birge and J. Zubieta, *Inorg. Chem.*, 1999, **38**, 5484.

13 N. A. Khan, N. Baber, M. Z. Iqbal and M. Mazhar, *Chem. Mater.*, 1993, **5**, 1283.

14 S. I. Stupp and P. V. Braun, *Science*, 1997, **277**, 1242.

15 S. Ayyappan, G. Diaz de Delgado, A. K. Cheetham, G. Férey and C. N. R. Rao, *J. Chem. Soc., Dalton Trans.*, 1999, 2905.

16 S. R. Batten and R. Robson, *Angew. Chem., Int. Ed.*, 1998, **37**, 1460 and references therein.

17 Some representative references from leading researchers in the field of coordination polymers: (*a*) M. J. Zaworotko, *Chem. Soc. Rev.*, 1994, **23**, 283; (*b*) H. Gudbjartson, K. Biradha, K. M. Poirier and M. J. Zaworotko, *J. Am. Chem. Soc.*, 1999, **121**, 2599; (*c*) B. F. Abrahams, P. A. Jackson and R. Robson, *Angew. Chem., Int. Ed.*, 1998, **37**, 2656; (*d*) L. Carlucci, G. Ciani, D. M. Proserpio and A. Sironi, *Inorg. Chem.*, 1998, **37**, 5941; (*e*) O. M. Yaghi, H. Li, C. Davis, D. Richardson and T. L. Groy, *Acc. Chem. Res.*, 1998, **31**, 474; (*f*) S. Lopez and S. W. Keller, *Inorg. Chem.*, 1999, **38**, 1883; (*g*) M. Kondo, T. Okubo, A. Asami, S. Noro, T. Yoshitomi, S. Kitagawa, T. Ishii, H. Matsuzaka and K. Seki, *Angew. Chem., Int. Ed.*, 1999, **38**, 140; (*h*) D. M. L. Goodgame, D. A. Grachvogel and D. J. Williams, *Angew. Chem., Int. Ed.*, 1999, **38**, 153; (*i*) C. V. K. Sharma and R. D. Rogers, *Chem. Commun.*, 1999, 83; (*j*) M. Fujita, Y. J. Kwon, S. Washizu and K. Ogura, *J. Am. Chem. Soc.*, 1994, **116**, 1151; (*k*) M. A. Withersby, A. J. Blake, W. R. Champness, P. Hubberstey, W.-S. Li and M. Schröder, *Angew. Chem., Int. Ed. Engl.*, 1997, **37**, 2327; (*l*) A. J. Blake, S. J. Mill, P. Hubberstey and W.-S. Li, *J. Chem. Soc., Dalton Trans.*, 1998, 909; (*m*) J. S. Moore and S. Lee, *Chem. Ind. (London)*, 1994, **14**, 556; (*n*) A. Mayr and J. Guo, *Inorg. Chem.*, 1999, **38**, 921.

18 Siemens SMART Software Reference Manual, Siemens Analytical X-Ray Instruments, Inc., Madison, Wisconsin, 1994.

19 G. M. Sheldrick, SADABS, Program for Empirical Absorption Corrections, University of Göttingen, Germany, 1996.

20 G. M. Sheldrick, SHELXL96, Program for the Refinement of Crystal Structures, University of Göttingen, Germany, 1996.

21 J. Gopalakrishnan, *Chem. Mater.*, 1995, **7**, 1265.

22 A. Stein, S. W. Keller and T. E. Mallouk, *Science*, 1993, **257**, 1558.

23 D. J. Chesnut, D. Hagrman, P. J. Zapf, R. P. Hammond, R. LaDuca, Jr., R. C. Haushalter and J. Zubieta, *Coord. Chem. Rev.*, 1999, **190–192**, 757.

24 D. Hagrman, P. J. Zapf and J. Zubieta, *Angew. Chem., Int. Ed.*, 1999, **38**, 3165.

25 A. G. Sharpe, *The Chemistry of Cyano Complexes of the Transition Metals*, Academic Press, New York, 1976.

26 D. T. Cromer, *J. Phys. Chem.*, 1957, **61**, 1388.

27 D. T. Cromer and A. C. Larson, *Acta Crystallogr.*, 1962, **15**, 397.

28 C. Kappenstein and R. P. Hugel, *Inorg. Chem.*, 1977, **16**, 250.

29 G. A. Bowmaker, H. Hartl and V. Urban, *Inorg. Chem.*, 2000, **39**, 4548.

30 F. B. Stocker, T. P. Staeva, C. M. Rienstra and D. Britton, *Inorg. Chem.*, 1999, **38**, 984.

31 S. Kroeker, R. E. Wasylishen and J. V. Hanna, *J. Am. Chem. Soc.*, 1999, **121**, 1582.

32 D. Cooper and R. A. Plane, *Inorg. Chem.*, 1966, **5**, 2209.

33 J. C. Dyason, P. C. Healy, L. M. Englehardt, C. Pakawatchai, V. A. Patrick and A. H. White, *J. Chem. Soc., Dalton Trans.*, 1985, 839.